

Selecting Energy Efficient Inputs using Graph Structure

Isaac Klickstein and Francesco Sorrentino *Senior Member, IEEE*

Abstract—Selecting appropriate inputs for systems described by complex networks is an important but difficult problem that largely remains open in the field of control of networks. Recent work has proposed two methods for energy efficient input selection; a gradient based heuristic and a greedy approximation algorithm. We propose here an alternative method for input selection based on the analytic solution of the controllability Gramian of simple graphs that appear as subgraphs in complex networks and facility location problems. The method presented is especially applicable for large networks where one is interested in controlling only a small number of outputs, or target nodes, for which current methods may not be practical. Our approach appears to be competitive to existing algorithms, while presenting computational advantages.

Index Terms—Enter key words or phrases in alphabetical order, separated by commas. For a list of suggested key words, send a blank e-mail to keywords@ieee.org or visit http://www.ieee.org/organizations/pubs/ani_prod/keyrd98.txt

I. INTRODUCTION

Many of the systems we interact with every day are described by complex networks such as social media [1], the power grid [2], [3], the world wide web [4], and our own biology [5]. As our ability to describe these complex networked systems improves, attention has increasingly turned to our ability to influence, or control, these systems with external signals. For example, targeted media campaigns (both beneficial and malicious) on social media platforms have proven to be incredibly effective [6], or as our knowledge of human pharmacology grows, multi-drug multi-target therapies become viable for drug developers [7]. While the dynamics of each of these systems are quite different, the first step toward influencing any of them requires a choice of where one should apply the external signal. This choice is integral to the effectiveness of the proposed intervention.

Here, we focus on linear systems as, at least over short time scales, continuous nonlinear systems can be approximated as linear [8], [9]. The problem of selecting the fewest number of control signals to ensure a complex network is controllable has been addressed in many different frameworks such as structural controllability [10], exact controllability [11], and output controllability [12]–[14]. While the minimum number of inputs is sufficient to ensure controllability, applying this minimum control may lead to extremely ill-conditioned systems of equations [15]–[18]. Instead, more recently, *efficient*

This work was supported by the National Science Foundation through Grant No. 1727948 and Grant CRISP-1541148.

I. Klickstein is with the Department of Mechanical Engineering, University of New Mexico, Albuquerque, NM 87131 USA (e-mail: iklick@unm.edu).

F. Sorrentino is with the Department of Mechanical Engineering, University of New Mexico, Albuquerque NM 87131 USA (e-mail: fsorrent@unm.edu).

control problems have garnered interest which look to minimize a control energy metric while constraining the number of control inputs [19]. The selection of the number of control inputs and their distribution throughout the complex network are vitally important to the feasibility and the efficiency of a control action.

Efficient controllability problems, unlike minimum controllability problems, minimize a metric on the control energy while constraining the number of control inputs [19]. Efficient control problems have previously been shown to be NP hard [20], [21] by mapping it to the Hitting Set problem following [22]. This result removes the possibility of any polynomial time algorithm to find the optimal solution. Instead, we must turn to heuristic methods and approximation algorithms.

One heuristic, called the projected gradient method, has been proposed in a series of papers [23]–[25] which differentiates the controllability Gramian with respect to the control input matrix assuming each input can be attached to every node in the network. The result is then rounded by replacing the columns of the found dense solution with versors where each versor is chosen to have its single nonzero component to be the entry of largest magnitude (which the authors call the key component analysis). In this paper, we compare our algorithm to a version of the above idea which uses a *probabilistic projection* [26] to avoid the rounding step required.

A number of control energy metrics were shown to be *submodular set functions* on the power set of the nodes [19], [27]. Greedy algorithms have a long known approximation guarantee when minimizing submodular set functions [28]. We compare our method to a greedy algorithm to minimize one of the control metrics shown to be submodular. More sophisticated extensions [20], [21] that expand on the greedy algorithm to handle some numerical difficulties have been developed but were not explicitly stated to be effective for the target control problem. The two main drawbacks of greedy algorithms to minimize control energy metrics are that (i) they require computing and storing many controllability Gramians which are expensive to compute [29], [30] and (ii) they may require finding properties such as the Gramian's determinant which is difficult when these are ill-conditioned matrices [17].

Following recent work on deriving analytic expressions for the control energy for lattice networks [31]–[34] we present here a new heuristic method that performs well for the target control problem. Our novel approach is broken into two parts. In the first half of the paper we derive the control energy of a model graph that represents two important quantities; graph distance and graph redundancy. The second half of the paper maps the input selection problem to the *facility location problem*, a well known integer linear programming problem

from the operations research literature. The cost matrix used in our method is created using the pair-wise surrogate cost developed in the first half.

In the next section, we present preliminaries about graphs, the controllability Gramian, and the facility location problem. We first obtain an analytic expression for the control energy of a particular model network, which we then exploit to derive a new heuristic method to solve the driver node selection problem in arbitrary networks. In the third section, we present results comparing our method to two published methods; (i) a greedy algorithm [19] and (ii) the L_0 -norm constraint based projected gradient method (LPGM), that attempt to solve the input allocation problem.

II. PRELIMINARIES

Graphs are denoted $\mathcal{G} = (\mathcal{V}, \mathcal{E})$ which consist of $|\mathcal{V}| = n$ nodes and edges $(v_j, v_k) \in \mathcal{E}$ which may be read as ‘from node v_j to node v_k .’ Unless otherwise stated, all graphs considered here are assumed to be directed. The set of neighbors of a node v_j , denoted \mathcal{N}_j , is defined as the set of nodes v_k such that $(v_k, v_j) \in \mathcal{E}$. We do not include any loops, that is an edge (v_j, v_j) , in the set of edges, as loops are treated separately. A graph may be represented as an adjacency matrix, $A \in \mathbb{R}^{n \times n}$, which has elements $A_{j,k} > 0$ if $(v_k, v_j) \in \mathcal{E}$ and $A_{j,k} = 0$ otherwise. The diagonal of the matrix A , $A_{j,j} < 0$, $j = 1, \dots, n$, represent the loops present at each node. In this paper, we assume *uniform edge weights* and *uniform loop weights*, that is, edge weights are equal, $A_{j,k} = A_{j',k'}$ for all $(v_j, v_k), (v_{j'}, v_{k'}) \in \mathcal{E}$ and $(v_{j'}, v_{k'}) \in \mathcal{E}$ and all loop weights are equal, $A_{j,j} = A_{k,k}$, for all $j, k = 1, \dots, n$. The edge weight is denoted $\gamma > 0$ and the loop weight is denoted $-\nu < 0$.

A. Graph Symmetries

A permutation of the graph nodes is a bijection $\pi: \mathcal{V} \mapsto \mathcal{V}$ that can be thought of as ‘shuffling’ the nodes. After applying a permutation, the set resulting set of edges, \mathcal{E}^π , consists of edges $(\pi(v_j), \pi(v_k)) \in \mathcal{E}^\pi$ if and only if $(v_j, v_k) \in \mathcal{E}$. A permutation is a symmetry if $\mathcal{E}^\pi = \mathcal{E}$, that is, the permutation does not alter the set of edges.

A permutation π can also be expressed as a matrix, $P \in \{0, 1\}^{n \times n}$, with elements $P_{j,k} = 1$ if $\pi(v_j) = v_k$ and $P_{j,k} = 0$ otherwise. Applying the permutation to the adjacency matrix yields the permuted adjacency matrix $A^\pi = PAP^T$. If π is a symmetry then $A^\pi = A$ (assuming uniform edge weights and loop weights as specified above).

The set of all symmetries along with function composition form the *automorphism group* of a graph, denoted $\text{Aut}(\mathcal{G})$. The automorphism group induces a partition of the nodes, defined as the orbits of the graph, $\mathcal{O} = \{\mathcal{O}_1, \dots, \mathcal{O}_q\}$, where two nodes $v_j, v_k \in \mathcal{O}_\ell$ if and only if there exists a symmetry π that maps $\pi(v_j) = v_k$. With the automorphism group, a graph can be compressed to its *quotient graph*, $\mathcal{Q} = (\mathcal{O}, \mathcal{F})$, where each orbit is a node in the quotient graph, and the edges $(\mathcal{O}_j, \mathcal{O}_k) \in \mathcal{F}$ represent those pairs of orbits for which there exists edges passing from the nodes in \mathcal{O}_j to the nodes in \mathcal{O}_k .

The orbit indicator matrix, $E \in \{0, 1\}^{n \times q}$, has elements $E_{j,k} = 1$ if node $v_j \in \mathcal{O}_k$ and $E_{j,k} = 0$ otherwise. The adjacency

matrix of the quotient graph, $A^Q \in \mathbb{R}^{q \times q}$, can be found by applying the orbit indicator matrix,

$$A^Q = E^\dagger AE \quad (1)$$

where the superscript \dagger denotes the Moore-Penrose pseudoinverse, defined as $E^\dagger = (E^T E)^{-1} E^T$. The elements of the quotient graph adjacency matrix, $A_{j,k}^Q$, are equal to the number of neighbors of a node $v_\ell \in \mathcal{O}_j$ that are in \mathcal{O}_k (multiplied by the uniform edge weight γ).

A useful concept used at the end of this section is the *reduced automorphism group* that arises when some nodes are not permitted to be permuted by any symmetry. Denote this forbidden subset $\mathcal{D} \subseteq \mathcal{V}$. The reduced automorphism group, $\text{Aut}^{\mathcal{D}}(\mathcal{G})$, consists of those symmetries π such that $\pi(v_j) = v_j$ for all $v_j \in \mathcal{D}$.

B. Minimum Control Energy

This paper is mainly concerned with dynamical processes defined on graphs. We are able to influence the dynamics through a subset of the nodes, $\mathcal{D} \subseteq \mathcal{V}$, defined as the $|\mathcal{D}| = m$ *driver nodes*. The driver node set can be represented as a matrix, $B \in \{0, 1\}^{n \times m}$, where each column of B has a single nonzero element corresponding to a driver node. An independent, external, control input, denoted $u_\ell(t)$, $\ell = 1, \dots, m$, is assigned to each driver node $v_\ell \in \mathcal{D}$. A time-varying state is assigned to each node, $x_j(t)$, $j = 1, \dots, n$, that is governed by the linear differential equation,

$$\dot{x}_j(t) = A_{j,j}x_j(t) + \sum_{v_k \in \mathcal{N}_j} A_{j,k}x_k(t) + \sum_{\ell=1}^m B_{j,\ell}u_\ell(t) \quad (2)$$

An initial condition is assigned to each node at time $t = 0$, $x_j(0) = x_{j,0}$. The set of p target nodes, denoted $\mathcal{T} \subseteq \mathcal{V}$, are those whose states we would like to drive to a particular value at some final time $t = t_f$. The set of target nodes can also be represented as a matrix, $C \in \{0, 1\}^{p \times n}$, where each row has a single nonzero element corresponding to a target node. We would like to determine the control inputs that drive the target nodes from their initial conditions to the desired final states that is minimum in their \mathcal{L}_2 norm.

$$\begin{aligned} \min \quad & J = \frac{1}{2} \int_0^{t_f} \|u(t)\|_2^2 dt \\ \text{s.t.} \quad & \dot{x}(t) = Ax(t) + Bu(t) \\ & x(0) = x_0, \quad Cx(t_f) = y_f \end{aligned} \quad (3)$$

This optimal control problem has a unique solution if and only if the triplet (A, B, C) is *output controllable*. The solution of this optimal control problem can be expressed as a quadratic form.

$$\begin{aligned} J^* &= \frac{1}{2} (y_f - Ce^{At_f}x_0)^T (CW(t_f)C^T)^{-1} (y_f - Ce^{At_f}x_0) \\ &= \frac{1}{2} \beta^T \bar{W}^{-1}(t_f) \beta \end{aligned} \quad (4)$$

The symmetric positive semi-definite matrix $W(t_f) \in \mathbb{R}^{n \times n}$ is the solution of the *differential Lyapunov equation*,

$$\dot{W}(t) = AW(t) + W(t)A^T + BB^T, \quad W(0) = O_n \quad (5)$$

If the triplet (A, B, C) is output controllable, then the matrix $CW(t_f)C^T$ is positive definite.

Definition 1 (Output Controllability). *The triplet (A, B, C) is output controllable if for every vector $x_0 \in \mathbb{R}^n$, vector $y_f \in \mathbb{R}^p$ and positive real name $t_f > 0$, there exists a control input $u : \mathbb{R}^+ \mapsto \mathbb{R}^m$ such that the solution of the system in Eq. (2) satisfies $y_f = Cx(t_f)$ at time $t = t_f$.*

Theorem 1 (Output Controllability Gramian [35]). *If a triplet (A, B, C) is output controllable then the output controllability Gramian, $CW(t_f)C^T$, is positive definite.*

If the matrix A is Hurwitz, that is, all of its eigenvalues lie on the left hand side of the complex plane, then there exists a unique stable fixed point of Eq. (5) which can be found by solving the algebraic Lyapunov equation.

$$O_n = AW(\infty) + W(\infty)A^T + BB^T \quad (6)$$

If the final t_f is large enough, then the algebraic Lyapunov equation may be a suitable substitute for the time-varying controllability Gramian found by integrating Eq. (5) forward in time. One is also able to use the solution of Eq. (6) to find the finite-time Gramian that evolves according to Eq. (5) using its formal solution.

$$\begin{aligned} W(t) &= \int_0^t e^{A\tau} BB^T e^{A^T \tau} d\tau \\ &= \int_0^\infty e^{A\tau} BB^T e^{A^T \tau} d\tau - \int_t^\infty e^{A\tau} BB^T e^{A^T \tau} d\tau \quad (7) \\ &= W(\infty) - e^{At} \int_t^\infty e^{A(\tau-t)} BB^T e^{A^T(\tau-t)} d\tau e^{A^T t} \\ &= W(\infty) - e^{At} W(\infty) e^{A^T t} \end{aligned}$$

Theorem 2 (Symmetries in the Gramian [32]). *Symmetries in the graph from which the adjacency matrix A was constructed can be witnessed in the values of the controllability Gramian. If two nodes $v_j, v_{j'} \in \mathcal{O}_\ell$ and another two nodes $v_k, v_{k'} \in \mathcal{O}_{\ell'}$, then the elements of the Gramian $W_{j,k}(t) = W_{j',k'}(t)$.*

In the following, define the driver node reduced automorphism group, $\text{Aut}^{\mathcal{D}}(\mathcal{G})$ so no driver node may be permuted by any symmetry. All mentions of orbit indicator matrix or quotient graph refer to those matrices and graphs induced by the driver node reduced automorphism group.

Rather than solving for the controllability Gramian, it may be more useful to compute the controllability Gramian for the quotient graph,

$$W^Q(t) = A^Q W^Q(t) + W^Q(t) A^{Q^T} + B^Q B^{Q^T} \quad (8)$$

where if $v_j \in \mathcal{O}_{j'}$ and $v_k \in \mathcal{O}_{k'}$ then $W_{j,k}(t) = W_{j',k'}^Q(t)$. Thus, if $W^Q(t)$ is known, we can ‘expand’ the result to determine $W(t)$.

C. Directed Balloon Graph

It has previously been shown [32], [34] that the optimal cost for the single driver node and single target node problem ($m = 1$ and $p = 1$) is intimately related to the structure of a graph. Two properties were shown to be important, the

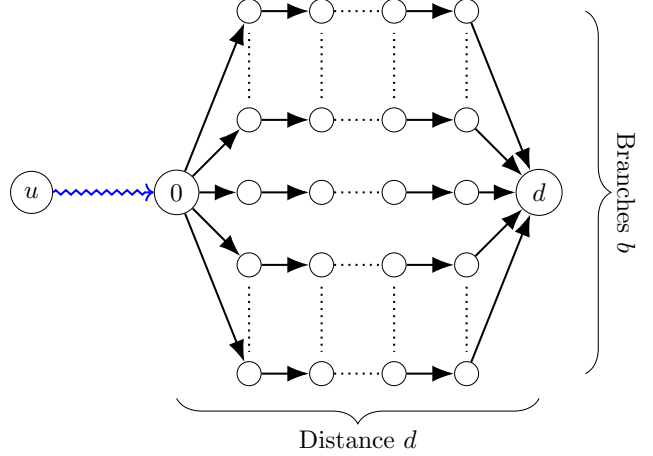


Fig. 1. A diagram of the directed balloon graph. There is a single driver node, labeled v_0 , then b parallel, disjoint paths of length d to the terminal node, labeled v_d . All edges have uniform weight γ and loop weight $-v$. A directed balloon graph can be completely defined by the two integers, d and b .

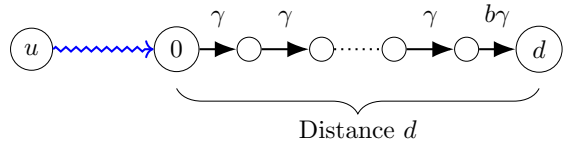


Fig. 2. A diagram of the quotient graph of the balloon graph. This graph is a directed path graph of uniform edge weight γ and uniform loop weight $-v$, except for the right-most edge which has weight $b\gamma$.

distance between the driver node and target node, $d_{j,k}$, and the number of nodes that lie along the shortest paths.

Definition 2 (Distance). *A path of length d is a sequence of d edges, $(v_{\ell,0}, v_{\ell,1}), (v_{\ell,1}, v_{\ell,2}), \dots, (v_{\ell_{d-1}}, v_{\ell_d})$. The distance from node v_j to node v_k is the length of the shortest path such $j = \ell_1$ and $k = \ell_d$.*

Definition 3 (Redundancy). *Let $\mathcal{V}_{j,k}$ be the number of nodes that lie along a shortest path from node v_j to node v_k .*

$$\mathcal{V}_{j,k} = \{v_\ell \in \mathcal{V} \mid d_{j,\ell} + d_{\ell,k} = d_{j,k}\} \quad (9)$$

The redundancy between a pair of nodes, $v_j, v_k \in \mathcal{V}$, whose distance apart is $d_{j,k} \geq 2$, is,

$$r_{j,k} = \frac{|\mathcal{V}_{j,k}| - 2}{d_{j,k} - 1} \quad (10)$$

A model that captures these two properties is the *directed balloon graph* that consists of two end nodes, labeled v_0 and v_d , and b disjoint directed paths from node v_0 to node v_d [32], [33]. A single control input is attached to node v_0 while v_d is the single target node. Each edge is assumed to have uniform weight $\gamma > 0$ and each loop has uniform weight $-v < 0$. The driver node v_0 and target node v_d are separated by distance $d_{0,d} = d$ and, from the definition of redundancy in Eq. (10), $r_{0,d} = b$. The quotient graph is a directed path graph with

$W_{0,d}(t)$	$W_{1,d}(t)$	\cdots	$W_{d-1,d}(t)$	$W_{d,d}(t)$
$W_{0,d-1}(t)$	$W_{1,d-1}(t)$	\cdots	$W_{d-1,d-1}(t)$	$W_{d,d-1}(t)$
\vdots	\vdots	\ddots	\vdots	\vdots
$W_{0,1}(t)$	$W_{1,1}(t)$	\cdots	$W_{d,0}(t)$	$W_{d,1}(t)$
$W_{0,0}(t)$	$W_{1,0}(t)$	\cdots	$W_{d-1,0}(t)$	$W_{d,0}(t)$

Fig. 3. Layout of the controllability Gramian of the quotient graph of the balloon graph in Fig. 2. The important entries are the origin, $W_{0,0}(t)$, the boundaries $W_{j,0}(t)$ and $W_{0,k}(t)$, $1 \leq j, k < d$, and the interior elements $W_{j,k}(t)$, $1 \leq j, k < d$. Finally, in the gray shaded region, are the elements for which the final edge weight of $b\gamma$ appears.

uniform edge weights γ and loop weights $-v$ except for the last edge, (v_{d-1}, v_d) , which has edge weight $b\gamma$.

D. Gramian of the Balloon Graph

The controllability Gramian of the graph in Fig. 2 is determined to better understand the role of distance and redundancy in control energy.

Theorem 3 (Controllability Gramian of the Directed Path Graph). *The controllability Gramian of the graph in Fig. 2 can be found by specializing Eq. (8). The entry we are most interested in is the diagonal element $W_{d,d}(t_f)$ as the optimal cost is equal to,*

$$\begin{aligned} J^* &= \frac{\beta^2}{2} \frac{1}{W_{d,d}(t_f)} \\ &= \frac{\beta^2}{2} \frac{2v}{b^2} \left(\frac{2v}{\gamma} \right)^{2d} \frac{(d!)^2}{(2d)!} \left[1 - e^{2vt_f} \sum_{k=0}^{2d} \frac{(2vt_f)^k}{k!} \right]^{-1} \end{aligned} \quad (11)$$

Proof. As the Gramian is computed for the quotient graph shown in Fig. 2 whose indices start at 0, the same is done in the controllability Gramian. Specifically, the entries of the Gramian start at $W_{0,0}(t)$ and grow outwards to $W_{d,d}(t)$, $d > 0$. The layout of the Gramian entries is shown in Fig. 3. The proof is broken into two parts; first the elements $W_{j,k}(t)$ for $0 \leq j, k < d$ are found, and second the boundary elements, $W_{d,k}(t)$ and $W_{j,d}(t)$, are found.

For the elements $W_{j,k}(t)$, $0 \leq j, k < d$, the differential

Lyapunov equation can be written as the following system of equations where all initial conditions are zero.

$$\begin{aligned} \dot{W}_{0,0}(t) &= -2vW_{0,0}(t) + 1 \\ \dot{W}_{j,0}(t) &= -2vW_{j,0}(t) + \gamma W_{j-1,0}(t), \quad 1 \leq j < d \\ \dot{W}_{0,k}(t) &= -2vW_{0,k}(t) + \gamma W_{0,k-1}(t), \quad 1 \leq k < d \\ \dot{W}_{j,k}(t) &= -2vW_{j,k}(t) + \gamma W_{j-1,k}(t) + \gamma W_{j,k-1}(t), \quad 1 \leq j, k < d \end{aligned} \quad (12)$$

From symmetry, $W_{j,0}(t) = W_{0,j}(t)$, so only one set of the boundary elements in Eq. (12) must be determined. As every equation in Eq. (12) is linear, the Laplace transform is taken of the system where $V(s) = \mathcal{L}\{W(t)\}$.

$$\begin{aligned} sV_{0,0}(s) &= -2vV_{0,0}(s) + \frac{1}{s} \\ sV_{j,0}(s) &= -2vV_{j,0}(s) + \gamma V_{j-1,0}(s) \\ sV_{0,k}(s) &= -2vV_{0,k}(s) + \gamma V_{0,k-1}(s) \\ sV_{j,k}(s) &= -2vV_{j,k}(s) + \gamma V_{j-1,k}(s) + \gamma V_{j,k-1}(s) \end{aligned} \quad (13)$$

The origin element is immediately determined to be,

$$V_{0,0}(s) = \frac{1}{s(s+2v)}. \quad (14)$$

The remaining elements are found using a generating function, denoted,

$$\hat{V}(x, y; s) = \sum_{j,k=0,1,\dots} V_{j,k}(s) x^j y^k. \quad (15)$$

Along the $k=0$ boundary, the elements can be found by setting $y=0$ so that,

$$\hat{V}(x, 0; s) = \sum_{j=0,1,\dots} V_{j,0}(s) x^j \quad (16)$$

Multiplying the second line of Eq. (13) by x^j and summing over all non-negative j yields,

$$\begin{aligned} (s+2v) \sum_{j=0,1,\dots} V_{j+1,0}(s) x^j &= \gamma \sum_{j=0,1,\dots} V_{j,0}(s) x^j \\ \frac{s+2v}{x} (\hat{V}(x, 0; s) - V_{0,0}(s)) &= \gamma \hat{V}(x, 0; s) \\ \hat{V}(x, 0; s) &= \frac{s+2v}{s+2v-\gamma x} V_{0,0}(s) \end{aligned} \quad (17)$$

Define $\rho(s) = \frac{\gamma}{s+2v}$ so that the boundary elements can more succinctly be written as,

$$\begin{aligned} \hat{V}(x, 0; s) &= \frac{1}{1-\rho(s)x} V_{0,0}(s) \\ &= V_{0,0}(s) \sum_{j \geq 0} \rho^j(s) x^j, \end{aligned} \quad (18)$$

which implies the boundary elements are,

$$V_{j,0}(s) = \frac{1}{s(s+2v)} \left(\frac{\gamma}{s+2v} \right)^j. \quad (19)$$

In turn, from symmetry, the other boundary must have elements $V_{0,k}(s) = \frac{1}{s(s+2v)} \left(\frac{\gamma}{s+2v} \right)^k$. The interior elements are

found using the two variable generating function.

$$\begin{aligned}
\hat{V}(x, y; s) &= \frac{1}{1 - \rho(s)(x+y)} V_{0,0}(s) \\
&= V_{0,0}(s) \sum_{\ell \geq 0} \left(\frac{\gamma}{s+2v} \right)^\ell (x+y)^\ell \\
&= V_{0,0}(s) \sum_{\ell \geq 0} \left(\frac{\gamma}{s+2v} \right)^\ell \sum_{a=0}^{\ell} \binom{\ell}{a} x^{\ell-a} y^a \\
&= V_{0,0}(s) \sum_{j,k \geq 0} \binom{j+k}{k} \left(\frac{\gamma}{s+2v} \right)^{j+k} x^j y^k
\end{aligned} \tag{20}$$

The interior elements of the controllability Gramian can be read off as the j, k 'th coefficient, $0 \leq j, k < d$,

$$V_{j,k}(s) = \frac{1}{s(s+2v)} \left(\frac{\gamma}{s+2v} \right)^{j+k} \binom{j+k}{k} \tag{21}$$

With all elements now determined for $j, k < d$ we move to the final layer. First, the element $V_{d,0}(s)$ is determined, then the elements $V_{d,j}(s)$ for $1 \leq j < d$, and then finally $V_{d,d}(s)$.

$$\begin{aligned}
V_{d,0}(s) &= \frac{b\gamma}{s+2v} V_{d-1,0}(s) \\
&= \frac{b}{s(s+2v)} \left(\frac{\gamma}{s+2v} \right)^d
\end{aligned} \tag{22}$$

Furthermore, it is straightforward to show that

$$V_{d,j}(s) = \frac{b}{s(s+2v)} \left(\frac{\gamma}{s+2v} \right)^{d+j} \binom{d+j}{d} \tag{23}$$

Finally, the element of interest in the Laplace domain can be computed,

$$\begin{aligned}
V_{d,d}(s) &= \frac{b\gamma}{s+2v} (V_{d-1,d}(s) + V_{d,d-1}(s)) \\
&= \frac{2b\gamma}{s+2v} \left(\frac{b}{s(s+2v)} \right) \left(\frac{\gamma}{s+2v} \right)^{2d-1} \binom{2d-1}{d} \\
&= \frac{b^2}{s(s+2v)} \left(\frac{\gamma}{s+2v} \right)^{2d} \binom{2d}{d}
\end{aligned} \tag{24}$$

The inverse Laplace transform of $V_{d,d}(s)$ is found by using identity 5.2.18 in [36] which states,

$$\mathcal{L}^{-1} \left\{ \frac{1}{s(s+a)^n} \right\} = \frac{1}{a^n} \left[1 - e^{-at} \sum_{k=0}^{n-1} \frac{(at)^k}{k!} \right] \tag{25}$$

Applying Eq. (25) to Eq. (24) yields the controllability Gramian element,

$$\begin{aligned}
W_{d,d}(t) &= \frac{b^2}{2v} \left(\frac{\gamma}{2v} \right)^{2d} \binom{2d}{d} \left[1 - e^{-2vt} \sum_{k=0}^{2d} \frac{(2vt)^k}{k!} \right] \\
&= \frac{b^2}{2v} \left(\frac{\gamma}{2v} \right)^{2d} \frac{(2d)!}{(d!)^2} [1 - r(t)]
\end{aligned} \tag{26}$$

As there is a single target node, the minimum control energy in Eq. (4) can be written,

$$J^* = \frac{\beta^2}{2} \frac{1}{W_{d,d}(t)} \tag{27}$$

Plugging Eq. (26) into Eq. (27) completes the proof. \square

Corollary 1. *In the $t \rightarrow \infty$ limit, the controllability Gramian element $W_{d,d}(t)$ approaches,*

$$J^* = \frac{\beta^2}{2} \lim_{t \rightarrow \infty} \frac{1}{W_{d,d}(t)} = \frac{\beta^2}{2} \frac{2v}{b^2} \left(\frac{2v}{\gamma} \right)^{2d} \frac{(d!)^2}{(2d)!} \tag{28}$$

Proof. Apply the final value theorem to Eq. (24) to show that,

$$\begin{aligned}
W_{d,d} &= \lim_{s \rightarrow 0} s \left[\frac{b^2}{s(s+2v)} \left(\frac{\gamma}{s+2v} \right)^{2d} \binom{2d}{d} \right] \\
&= \frac{b^2}{2v} \left(\frac{\gamma}{2v} \right)^{2d} \frac{(2d)!}{(d!)^2}
\end{aligned} \tag{29}$$

From Eq. (27), the result is immediate. \square

III. RESULTS

To apply the results discussed above to the optimal input selection problem, we return to the original optimal control problem in Eq. (3). The optimal input, $\mathbf{u}^*(t)$, is used to rewrite the same cost function using the solution in Eq. (4) but instead the set of driver nodes is taken to be the unknowns.

$$\begin{aligned}
\min_{\mathcal{D} \subset \mathcal{V}} \quad & J = \beta^T (CW(t_f)C^T)^{-1} \beta \\
\text{s.t.} \quad & |\mathcal{D}| = m \\
& \dot{W}(t) = AW(t) + W(t)A^T + BB^T, \quad W(0) = O_n
\end{aligned} \tag{30}$$

The B matrix in Eq. (30) is constructed from the set \mathcal{D} as described above. The optimization problem in Eq. (30) has been shown to be NP-hard [21], [22], along with a number of closely related problems, removing the possibility of a polynomial time algorithm.

Instead of minimizing the cost function in Eq. (30) directly, which depends on the particular control maneuver β , often a *general purpose* set of driver nodes is searched for instead which is found by introducing a *surrogate cost function*. In the remainder of this section, three surrogate cost functions are used; (i) a volume based metric [19], $-\log \det(\bar{W}(\infty))$, (ii) an expectation based quantity [26], $\text{Tr}(C^T \bar{W}^{-1}(t_f) C e^{At_f} e^{A^T t_f})$, and (iii) a pair-wise distance and redundancy based value using the results derived in the previous section. Methods developed to optimize the first two surrogate cost functions are summarized here, followed by the facility location problem (FLP) which we use to minimize the third surrogate cost function.

A. Greedy Algorithm [19]

The set of all control maneuvers capable of being performed with E units of energy forms a p -dimensional ellipsoid.

$$\mathcal{S} = \{ \beta \in \mathbb{R}^p \mid \beta^T \bar{W}^{-1}(t_f) \beta = E \} \tag{31}$$

The volume of this ellipsoid is known to be related to the determinant of the matrix $\bar{W}(t_f)$.

$$\log V(\mathcal{S}) = \log \left(\frac{\pi^{p/2}}{\Gamma(p/2+1)} \right) + \frac{1}{p} \log \det(\bar{W}(t_f)) \tag{32}$$

The logarithm is taken of the volume as the determinant of the controllability Gramian can fall below the floating point accuracy of double precision [17]. In [19], the cost function in Eq. (30) was replaced with the negative of Eq. (32) and it was shown to be a *submodular set function*. This cost is denoted,

$$\text{Vol}(\mathcal{D}) = -\log \det \bar{W}_{\mathcal{D}}. \quad (33)$$

A greedy algorithm that at each iteration adds the single node to the driver node set that improves the cost function the most has an approximation guarantee of 63% when the cost function is submodular [28].

By the definition of the matrix B we impose, the matrix product can be decomposed into the individual contributions of each driver node $BB^T = \sum_{v_k \in \mathcal{D}} e_k e_k^T$ where e_k is the unit vector with the single non-zero element corresponding to each driver node. This decomposition can be used to split the differential Lyapunov equation in Eq. (5) into the contribution of each driver node as well.

$$\begin{aligned} \dot{W}_k(t) &= AW_k(t) + W_k A^T + e_k e_k^T, \quad W_k(0) = O_n \\ W(t) &= \sum_{v_k \in \mathcal{D}} W_k(t) \end{aligned} \quad (34)$$

A greedy algorithm to minimize $\text{Vol}(\mathcal{D})$ over the powerset of the nodes could be applied directly assuming perfect arithmetic.

The difficulty of applying the greedy algorithm directly arises in two ways. The first difficulty is that storing all potential contributions of each driver node requires np^2 double precision variables which, if p is large, could be prohibitive. The second difficulty is computing $\text{Vol}(\mathcal{D})$ for the first few driver node sets as the Gramian is known to have extremely small (below double precision accuracy) eigenvalues when the number of target nodes is large relative to the number of driver nodes [18]. A proposed method [19] to handle the first few driver nodes replaces the evaluation of $\text{Vol}(\mathcal{D})$ with $-\text{rank}_{\text{num}}(\mathcal{D})$ where the function $\text{rank}_{\text{num}}(\cdot)$ computes the *numerical rank* of the output Gramian $\bar{W}_{\mathcal{D}}(t_f)$ [17]. This substitute is used until enough driver nodes have been added by the greedy algorithm to ensure the output controllability Gramian is of full numerical rank. Algorithm 2 in Appendix I shows this modified version where a flag is used to perform the switch from computing the rank to the determinant.

B. Projected Gradient Method [26]

Rather than choosing a particular control maneuver, let us assume that $\mathbf{y}_f = \mathbf{0}_p$ and \mathbf{x}_0 is an independent random variable with mean zero and variance one so that $\mathbb{E}[\mathbf{x}_0 \mathbf{x}_0^T] = I_n$. The expectation of the control maneuver can then be written [23],

$$X_f = \mathbb{E}[e^{A t_f} \mathbf{x}_0 \mathbf{x}_0^T e^{A^T t_f}] = e^{A t_f} e^{A^T t_f} \quad (35)$$

The expectation of the control energy over the control maneuvers is then optimized where $E : \mathbb{R}^{n \times m} \mapsto \mathbb{R}$ makes explicit the dependence of the energy on the input matrix B .

$$\begin{aligned} \min \quad & E(B) = \text{Tr}(C^T \bar{W}_B^{-1}(t_f) C X_f) \\ \text{s.t.} \quad & \bar{W}_B(t_f) = C \left[\int_0^{t_f} e^{A t} B B^T e^{A^T t} dt \right] C^T \\ & \|B\|_0 = m, \quad \text{rank}(B) = m \end{aligned} \quad (36)$$

The norm $\|B\|_0$ counts the number of nonzero elements and the constraint $\text{rank}(B) = m$ ensures each nonzero in B appears in a unique row and column. The main result that allows a gradient descent method to be used is the following derivative.

$$\begin{aligned} \frac{\partial E(B)}{B} &= -2 \int_0^{t_f} e^{A^T t} C^T \bar{W}_B^{-1}(t_f) C X_f \\ &\quad \times C^T \bar{W}_B^{-1}(t_f) C e^{A t} dt B \end{aligned} \quad (37)$$

Details of the algorithm are discussed in Appendix II. The gradient direction found in Eq. (37) will be *dense*, that is, most elements will be non-zero. The new matrix B , found by moving in the direction determined in Eq. (37), will then also be dense even if the original B is sparse. To compensate for this, a probabilistic projection is used, $\mathcal{P} : \mathbb{R}^{n \times m} \mapsto 2^{\mathcal{V}}$, that finds a set of nodes of cardinality m from a dense matrix. Details of the projection can be found in Algorithm 3 in Appendix II.

To make the cost in Eq. (36) comparable to the other methods described in this paper, define the expected control energy for a set of nodes to be,

$$\bar{E}(\mathcal{D}) = \text{Tr}(C^T \bar{W}_{\mathcal{D}}^{-1}(t_f) C X_f) \quad (38)$$

where $\bar{W}_{\mathcal{D}}(t_f) = C [\sum_{v_k \in \mathcal{D}} W_k(t_f)] C^T$ and $W_k(t_f)$ is defined in Eq. (34).

C. Facility Location Problems

The two methods presented above are important contributions to the input selection problem but they are both reliant on properties of the controllability Gramian rather than the structure of the system explicitly. The main result of this paper is a third approach to the input selection problem which exploits structural properties between each node and the set of target nodes in order to choose an energy efficient set of driver nodes.

Facility location problems (FLP) originally arose to address the problem of choosing distribution centers to accommodate demands while minimizing transportation costs [37]. Let there be p locations that must be supplied from m distribution centers selected from $n \geq m$ possible choices. The cost of supplying the j 'th location from the k 'th distribution center is denoted $c_{j,k}$. Each location is assumed to be supplied from a single distribution center. Let the binary variables $Y_j \in \{0, 1\}$, $j = 1, \dots, n$, be the possible distribution centers where $Y_j = 1$ if it is chosen to be a distribution center and $Y_j = 0$ otherwise. Let the binary variables $Z_{j,k} \in \{0, 1\}$, $j = 1, \dots, n$, $k = 1, \dots, p$, denote assignments so that if distribution center j supplies location k then $Z_{j,k} = 1$ and $Z_{j,k} = 0$ otherwise.

The FLP can be posed as an integer linear programming

(ILP) with binary variables.

$$\begin{aligned} \min \quad & \sum_{j=1}^n \sum_{k=1}^p Y_j Z_{j,k} c_{j,k} \\ \text{s.t.} \quad & \sum_{j=1}^n Y_j = m \\ & \sum_{j=1}^n Z_{j,k} = 1, \quad k = 1, \dots, p \\ & Z_{j,k} \leq Y_j, \quad j = 1, \dots, n, \quad k = 1, \dots, p \end{aligned} \quad (39)$$

The first constraint ensures that precisely m locations are chosen to be distribution centers. The second constraint ensures that each location to be supplied is assigned to a single distribution center. The third constraint ensures locations to be supplied are only assigned to distribution centers that are opened.

Even large instances ($n \approx 1000$) of the FLP stated as an ILP in Eq. (39) can be solved efficiently with ILP solvers such as the GNU Linear Programming Kit [38]. Moreover, recent efforts have developed specialized algorithms to approximately solve the FLP with an approximation guarantee [39]. Alternatives to the ILP should be used for very large problems. In the following section, the facility location problem is mapped to the input selection problem for a dynamical system described by a graph.

D. Pair-wise Cost

To apply the FLP formulation discussed in the previous section, let the locations to be supplied be the target nodes, \mathcal{T} , and the possible distribution centers be all of the nodes \mathcal{V} , from which the m driver nodes are selected. Without loss of generality, we assume that the $\mathcal{T} = \{v_j | j = 1, \dots, p\}$, that is, the first p nodes are selected to be the target nodes. For a pair of nodes, v_j and v_k , define $d_{j,k}$ to be the distance from node v_j to node v_k (see Def. 2) and define $r_{j,k}$ to be the redundancy from node v_j to node v_k (see Def. 3). The pair-wise cost is generated using the Gramian of the balloon graph in Eq. (11) and Stirling's approximation.

$$\begin{aligned} W_{k,k}^{ball} &= \frac{r_{j,k}^2}{2v} \left(\frac{\gamma}{2v} \right)^{2d_{j,k}} \frac{(2d_{j,k})!}{(d_{j,k}!)^2} \\ &\approx \frac{r_{j,k}^2}{2v} \left(\frac{\gamma}{2v} \right)^{2d_{j,k}} \frac{2\sqrt{\pi d_{j,k}} (2d_{j,k}/e)^{2d_{j,k}}}{\left(\sqrt{2\pi d_{j,k}} (d_{j,k}/e) \right)^{d_{j,k}}} \\ &= \left[\frac{2v}{r_{j,k}^2} \left(\frac{v}{\gamma} \right)^{2d_{j,k}} \sqrt{\pi d_{j,k}} \right]^{-1} \end{aligned} \quad (40)$$

Stirling's approximation for the factorial [40], $n! \approx \sqrt{2\pi n} (n/e)^n$, is used to reduce the approximation to the form in Eq. (40). The pair-wise cost that appears in Eq. (39) can then be written as,

$$c_{j,k} = \log \left(\frac{2v}{r_{j,k}^2} \left(\frac{v}{\gamma} \right)^{2d_{j,k}} \sqrt{\pi d_{j,k}} \right) \quad (41)$$

The main advantage of Eq. (41) over the other choices of cost in Eqs. (33) and (38) is that it only requires computing

the distances and redundancies between pairs of nodes instead of computing and then solving systems of equations with the controllability Gramian. The FLP cost associated with a set of driver nodes, \mathcal{D} , is determined by searching for the lowest cost assignment for each target node,

$$FLP(\mathcal{D}) = \sum_{k=1}^p \min_{v_j \in \mathcal{D}} c_{j,k} \quad (42)$$

For the pair-wise cost in Eq. (41) to perform well when compared to the two alternatives, there should be a monotonic relation between it and the other costs in Eq. (32) and Eq. (36). If this is true, then finding a set \mathcal{D} with a small $FLP(\mathcal{D})$ value should also have a small $\text{Vol}(\mathcal{D})$ and $\bar{E}(\mathcal{B})$ values as well.

To demonstrate this relationship, sets of nodes which satisfy $f - \varepsilon \leq FLP(\mathcal{D}) \leq f + \varepsilon$ for some small ε and desired cost f are determined using a hill climbing procedure shown in Algorithm 1. With the found set of nodes, the two other costs

Algorithm 1 Hill Climbing Procedure

Require: N a maximum number of allowed iterations, $\mathcal{G} = (\mathcal{V}, \mathcal{E})$ a directed graph, $\mathcal{T} \subseteq \mathcal{V}$ a set of target nodes, \hat{C} a desired cost, ε an acceptable threshold.
 $\mathcal{D}^{(0)}$ is initialized with m randomly selected nodes.
 $C^{(0)} \leftarrow FLP(\mathcal{D}^{(0)})$
 $k \leftarrow 1$
while $k < N$ **do**
 Choose $v_a \in \mathcal{D}^{(k-1)}$ and $v_b \notin \mathcal{D}^{(k-1)}$ randomly.
 Create $\bar{\mathcal{D}}^{(k)}$ by swapping v_a and v_b .
 $C^{(k)} \leftarrow FLP(\bar{\mathcal{D}}^{(k)})$
 if $\hat{C} - \varepsilon \leq C^{(k)} \leq \hat{C} + \varepsilon$ **then**
 $\mathcal{D}^{(k)} \leftarrow \bar{\mathcal{D}}^{(k)}$
 break
 else if $|\hat{C} - C^{(k)}| < |\hat{C} - C^{(k-1)}|$ **then**
 $\mathcal{D}^{(k)} \leftarrow \bar{\mathcal{D}}^{(k)}$
 else
 $\mathcal{D}^{(k)} \leftarrow \mathcal{D}^{(k-1)}$
 end if
end while
if $k = N$ **then**
 No set of nodes was found that satisfies the cost \hat{C} .
 An error flag should be returned.
end if

are also computed and we see a positive correlation. The relationship between the ellipsoid volume cost in Eq. (33) and the FLP cost in Eq. (42) and the expectation energy expression in Eq. (38) and the FLP cost is shown for four example graphs in Figs. 4 and 6, respectively. Each graph has $n = 300$ nodes, $p = 100$ target nodes selected randomly, and a driver node set of $m = 33$ nodes is determined. The four graphs' method of construction is described in the captions of Figs. 4 and 6. The log volume cost in Eq. (32) cost to minimize appears on the vertical axis of each plot while the FLP cost to minimize appears on the horizontal axis. From the trends in Fig. 4, it is clear that if we were to find the optimal set of driver nodes using the FLP formulation, that set of driver nodes would also be a competitive solution in the original optimization problem.

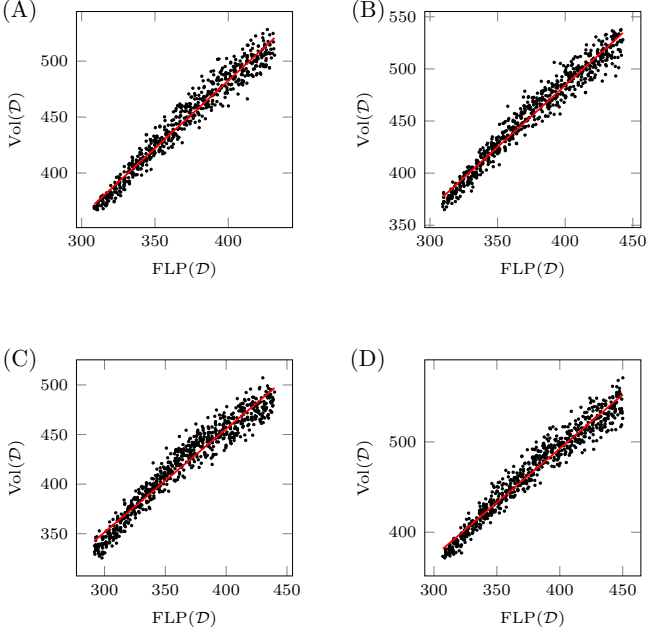


Fig. 4. Comparison of the volume based cost, $-\log \det(\bar{W}_D^T)$, and the pair-wise cost function $FLP(\mathcal{D})$. The graphs used for the analysis are (A) a k -regular graph with $k = 10$, (B) an Erdős-Rényi graph with $\kappa_{av} = 10$, (C) a Watts-Strogatz graph with average degree $\kappa_{av} = 8$ and (D) a graph with a power law degree distribution with exponent $\gamma = 3$ and average degree $\kappa_{av} = 10$ created using the configuration model. All graphs are directed with $n = 300$ nodes. The set of $p = 100$ targets are chosen randomly. The set of $m = 33$ driver nodes are determined using the hill climbing process described in the text and Algorithm 1 to achieve a desired value of $FLP(\mathcal{D})$. The four plots shown here are typical of all graphs examined, directed and undirected.

In the next section, the result found with the FLP method is compared to the greedy algorithm and the probabilistic gradient descent method mentioned previously.

E. Comparison to the Greedy Algorithm

To compare the FLP formulation described above and the greedy algorithm, we create 1000 graphs and compute the set of driver nodes returned by the greedy algorithm in Algorithm 2 and by solving the FLP in Eq. (39). In Fig. 5, 1000 graphs of the following types are used to make the comparison; 5(A) a k -regular graph with $k = 10$, 5(B) an Erdős-Rényi graph with $\kappa_{av} = 10$, 5(C) a Watts-Strogatz graph with average degree $\kappa_{av} = 8$ and 5(D) a graph with a power law degree distribution with exponent $\gamma = 3$ and average degree $\kappa_{av} = 10$ created using the configuration model. Each graph is undirected and is constructed with $n = 50$ nodes and $p = 20$ nodes are chosen randomly to be in the target node set \mathcal{T} . We look for a set of $m = 10$ driver nodes, \mathcal{D} , such that the cost function in Eq. (32) is minimized. The set of driver nodes returned using the FLP formulation, denoted \mathcal{D}_{FLP} , and the set of driver nodes returned by the modified greedy algorithm, denoted \mathcal{D}_{greedy} , are found for each graph and their costs are computed. The difference of their costs,

$$D_{greedy} = \log \det(\bar{W}_{FLP}^{-1}) - \log \det(\bar{W}_{greedy}^{-1}) \quad (43)$$

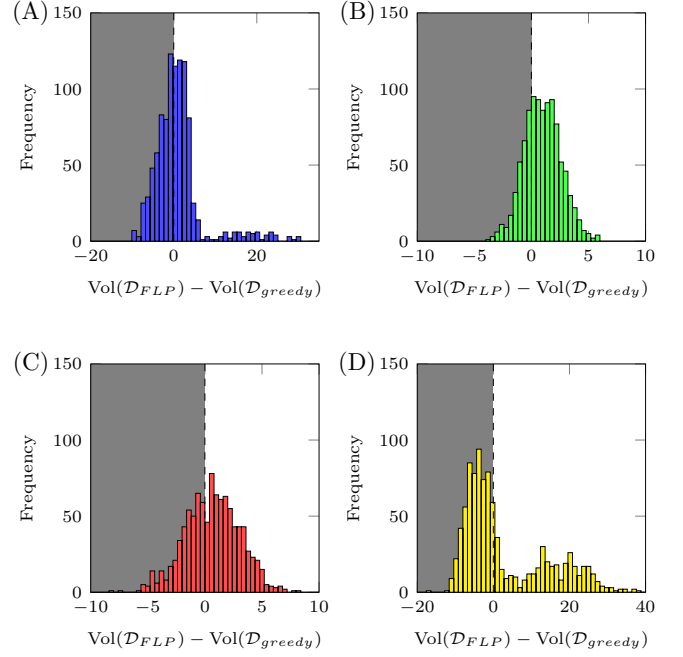


Fig. 5. Comparison of the performance of the FLP formulation with the greedy algorithm. Each panel computes the difference between $\text{Vol}(\mathcal{D}_{FLP})$ and $\text{Vol}(\mathcal{D}_{greedy})$ defined in Eq. (33). The four types of graphs used are (A) Erdős-Rényi graphs with $\kappa_{av} = 6$, (B) k -regular graphs with $k = 5$, (C) Watts-Strogatz graphs [41] with $p = 5\%$, and (D) graphs with a power-law distribution with exponent $\gamma = 3$ and $\kappa_{av} = 6$. Each graph has $n = 50$ nodes, $p = 20$ targets and $m = 10$ driver nodes are selected. All graphs are undirected. Each panel finds the set of driver nodes returned by the FLP formulation and the greedy algorithm and compares the returned cost. The grey background represents cases when the FLP formulation performs better and the white background represents cases when the greedy algorithm performs better.

is taken so that if $D_{greedy} < 0$, \mathcal{D}_{FLP} is more efficient while if $D > 0$, \mathcal{D}_{greedy} is more efficient. In Fig. 5, the cases when \mathcal{D}_{FLP} is more energy efficient are shown with a gray background while the cases when \mathcal{D}_{greedy} is more energy efficient are shown with a white background. We see that for some graph types (panels 5(A) and 5(D)), the FLP method performs better than the greedy algorithm more often, while for other graph types, the greedy algorithm performs better more often. Also, especially for the graphs with a power-law degree distribution in Fig. 5(D), the FLP method may perform very badly as seen by the second peak in the section of the plot with a white background. We hypothesize that this may be because the FLP cost treats each driver node target node pair independently and does not account for the fact one driver node may be assigned to many target nodes. Including this multiple target node assignment cost is the subject of future work.

F. Comparison to LPGM

The pair-wise cost in Eq. (42) is also correlated with the expectation cost used by LPGM in Eq. (36). A demonstration of this relation is shown in Fig. 6 for four types of graphs described in the caption. The two costs, $\bar{E}(\mathcal{D})$ and $FLP(\mathcal{D})$ are positively correlated as shown by the linear fitted line in red. A comparison of the performance of the FLP method and

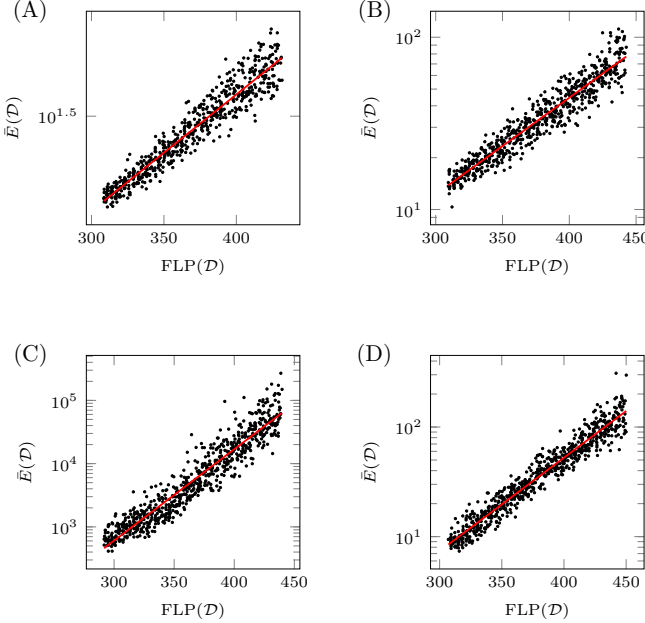


Fig. 6. Comparison of the expectation energy cost in Eq. (38) and the pairwise cost in Eq. (42). The graphs used for the analysis are (A) a k -regular graph with $k = 10$, (B) an Erdős-Rényi graph with $\kappa_{av} = 10$, (C) a Watts-Strogatz graph with average degree $\kappa_{av} = 8$ and (D) a graph with a power law degree distribution with exponent $\gamma = 3$ and average degree $\kappa_{av} = 10$ created using the configuration model. Each graph has $n = 300$ nodes, $p = 100$ targets chosen randomly, and $m = 33$ driver nodes which are to be chosen using the hill climbing procedure described in Alg. 1.

the LPGM heuristic for sets of four types of graphs is shown in Fig. 7. As in Fig. 5, bars in front of the gray background represent cases where the FLP algorithm returns more energy efficient driver node sets than the LPGM algorithm and vice versa for the bars with a white background. For the four types of graphs examined, we see that the FLP method and the LPGM heuristic either algorithm may perform better than the other, with some slight bias towards one or the other depending on the method. For other types of graphs, number of nodes, number of targets and number of drivers, one algorithm or the other may work better. The benefit of the FLP method is that it scales to larger problems better than the LPGM heuristic and it does not suffer from the same overflow/underflow issues as discussed in Appendix C.

IV. CONCLUSION

A novel method for the energy efficient selection of control inputs is presented based on graph structure. This is done in two steps; (i) the analytic calculation of the exact solution of the output controllability Gramian for a special model graph that captures the role of *redundant paths* and *distance* between a driver node and a target node and (ii) the application of the pair-wise cost computed in the *facility location problem* to choose driver nodes in a general graph. This approach is in contrast to the current available methods which rely on solving the Lyapunov equation many times, as well as computing properties of the output controllability Gramian which may be ill-conditioned. We see that finding efficient sets of control

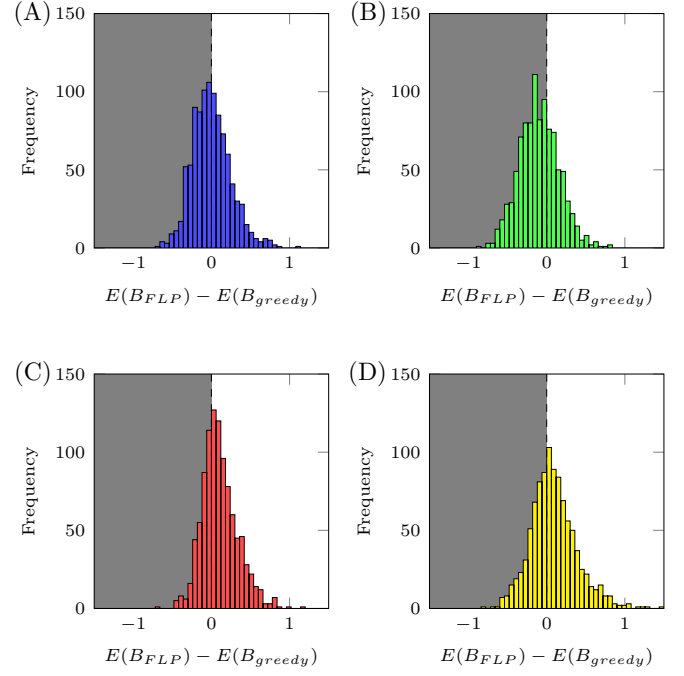


Fig. 7. A comparison of the performance between LPGM and FLP method for the expectation energy cost in Eq. (36) for 1000 realizations of the following four types of graphs. The four types of graphs used are (A) Erdős-Rényi graphs with $\kappa_{av} = 6$, (B) k -regular graphs with $k = 5$, (C) Watts-Strogatz graphs [41] with $p = 5\%$, and (D) graphs with a power-law distribution with exponent $\gamma = 3$ and $\kappa_{av} = 6$. All graphs have $n = 50$ nodes, $p = 20$ target nodes selected randomly, and $m = 10$ driver nodes are selected.

inputs using our structure based method is a competitive approach to the Gramian-based methods previously published, while our approach is computationally more efficient.

APPENDIX A GREEDY ALGORITHM

A greedy algorithm to find a set of nodes to assign to the driver node set to maximize the surrogate cost function in Eq. (32) is shown in Algorithm 2. In Algorithm 2, we include a flag so that the first iterations use the rank of the output controllability Gramian until at some iteration, the set of driver nodes selected so far ensure the output controllability Gramian has full *numerical rank*.

APPENDIX B \mathcal{L}_0 -CONSTRAINT PROJECTED GRADIENT METHOD

A published algorithm proposed to solve the input selection problem to which we compare the FLP method is the \mathcal{L}_0 -constrained projected gradient method (LPGM) [26]. The method combines the projected gradient method (PGM) [23], [42] which assumes all values in the B matrix with a *probabilistic projection*. The probabilistic projection in Algorithm 3 appears as a step, denote $B^{L0} \leftarrow \mathcal{P}(B)$ in the following gradient descent algorithm in Algorithm 4.

Algorithm 2 Greedy Minimization of a Set Function

Require: A desired set cardinality m , a state matrix A , a set of target nodes \mathcal{T} , a final time t_f (possibly ∞).

for $k = 1, \dots, n$ **do**

- Compute and store $CW_k(t_f)C^T$

end for

Initialize $\mathcal{D} \leftarrow \emptyset$, $\bar{W} \leftarrow O_p$, $k \leftarrow 0$.

$\text{flag} \leftarrow 1$

while $k < m$ **do**

- $f_{best} \leftarrow \infty$, $a_{best} \leftarrow -1$
- for** $j \in \mathcal{V} \setminus \mathcal{D}$ **do**

 - if** flag **then**
 - $f \leftarrow -\text{rank}(\bar{W} + CW_j(t_f)C^T)$
 - else**
 - $f \leftarrow -\log \det(\bar{W} + CW_j(t_f)C^T)$
 - end if**
 - if** $f < f_{best}$ **then**
 - $f \leftarrow f_{best}$, $a_{best} \leftarrow j$
 - end if**

end for

$\mathcal{D} \leftarrow \mathcal{D} \cup \{a_{best}\}$

$\bar{W} \leftarrow \bar{W} + CW_{a_{best}}(t_f)C^T$

if $\text{flag} \&& -C_{best} == p$ **then**

 - $\text{flag} \leftarrow 0$

end if

$k \leftarrow k + 1$

end while

return \mathcal{D}

Algorithm 3 Probabilistic Projection [26]

Require: $B \in \mathbb{R}^{n \times m}$

Require: $m_0 > 0$

$r_j \leftarrow \sum_{k=1}^m |B_{j,k}|$, $j = 1, \dots, n$

$\mathcal{I}_{candidate} \leftarrow \{j | r_j \text{ is one of the } m + m_0 \text{ largest values}\}$

$\mathcal{I}_{selected} \leftarrow \emptyset$

while $|\mathcal{I}_{selected}| < m$ **do**

- $p_j \leftarrow \begin{cases} r_j, & j \in \mathcal{I}_{candidate} \\ 0, & j \notin \mathcal{I}_{candidate} \end{cases}$, $j = 1, \dots, n$
- Choose j according to the probabilities in p .
- $\mathcal{I}_{selected} \leftarrow \mathcal{I}_{selected} \cup \{j\}$
- $\mathcal{I}_{candidate} \leftarrow \mathcal{I}_{candidate} \setminus \{j\}$

end while

$B^{L0} \leftarrow O_{n \times m}$

for $j \in \mathcal{I}_{selected}$ ($k = 1, \dots, m$) **do**

- $B_{j,k}^{L0} \leftarrow m r_j$

end for

$B^{L0} \leftarrow B^{L0} / \sum_{j \in \mathcal{I}_{selected}} r_j$

return B^{L0}

Algorithm 4 Projected Gradient Descent [26]

Require: Graph $\mathcal{G}(\mathcal{V}, \mathcal{E})$ with adj. matrix $A \in \mathbb{R}^{n \times n}$

Require: $B_0 \in \mathbb{R}^{n \times m}$

Require: $\mathcal{T} \subseteq \mathcal{V}$ (and corresponding $C \in \{0, 1\}^{p \times n}$)

Require: $\eta > 0$, $t_f > 0$, $K > 1$

$E_{best} \leftarrow \infty$

$X_f \leftarrow e^{At_f} e^{A^T t_f}$

for $k = 0, \dots, K$ **do**

- $B_k^{L0} \leftarrow \mathcal{P}(B_k)$
- $W \leftarrow \text{Lyap}(A, B_k^{L0} B_k^{L0T}, t_f)$
- $\bar{W} \leftarrow CWC^T$
- $E_k \leftarrow \text{Tr}(C^T \bar{W}^{-1} CX_f)$
- $R \leftarrow C^T \bar{W}^{-1} CX_f C^T \bar{W}^{-1} C$
- $W \leftarrow \text{Lyap}(A^T, R, t_f)$
- $\nabla E(B_k^{L0}) \leftarrow -2WB_k^{L0}$
- if** $E < E_{best}$ **then**

 - $E_{best} \leftarrow E$
 - $B_{best}^{L0} \leftarrow B_k^{L0}$
 - $B_{k+1} \leftarrow B_k^{L0} - \eta \nabla E(B_k^{L0})$

- else**
- $B_{k+1} \leftarrow B_k - \eta \nabla E(B_k^{L0})$
- end if**

end for

return $\mathcal{D} \leftarrow \mathcal{I}_{best}$

APPENDIX C

COMPUTATIONAL COST COMPARISON

In the paper, namely Figs. 5 and 7, we show that the FLP cost in Eq. (42) used in the ILP formulation in Eq. (39) can find competitive solutions to both the greedy algorithm with the volumetric cost in Eq. (33) and the LPGM heuristic with the expected energy cost in Eq. (38). While the FLP formulation does not clearly out-perform either of the other methods in all cases, it does avoid a numerical difficulty faced by both the greedy algorithm and the LPGM heuristic. In the greedy algorithm, we must first compute the output controllability Gramian for each potential driver nodes' contribution, which if every node is a viable candidate, using the Bartels-Stewart algorithm [43], requires $\mathcal{O}(n^4)$ work. At each step, k , for $k = 1, 2, \dots, m$, we must compute either the determinant (using a Cholesky decomposition) or the rank (using a rank revealing QR decomposition) for $(n-k+1) p \times p$ output controllability Gramians which both require $\mathcal{O}(p^3)$ work as we perform the comparison between each potential node to add to the set of driver nodes. Thus, the computational complexity of the whole greedy algorithm is $\mathcal{O}(nmp^3 + n^4)$.

The computational complexity of the LPGM heuristic, on its face, is less than the greedy algorithm, but the use of finite precision instead is the main barrier to applicability. To compute the descent direction, we must solve the following Lyapunov equation,

$$O = A^T Y + YA + R \quad (44)$$

for the square matrix Y where,

$$R = C^T \bar{W}_B^{-1} CX_f C^T \bar{W}_B^{-1} C \quad (45)$$

can have extremely large values due to the inverse of the output controllability Gramian appearing twice. As Eq. (44) is a linear equation, it can also be written as $\bar{A} \cdot \text{vec}(Y) = -\text{vec}(R)$ where $\text{vec}(\cdot)$ stacks the columns of a matrix into a vector and $\bar{A} = A^T \otimes I_n + I_n \otimes A$. Let $\|\cdot\|$ be a vector norm, then we know that,

$$\|\bar{A} \cdot \text{vec}(Y)\| = \|\text{vec}(R)\| \leq \|\bar{A}\| \cdot \|\text{vec}(Y)\| \quad (46)$$

where $\|\bar{A}\|$ is on the order of the maximum degree in the graph so that the norm of Y will be on the order of the norm of R , potentially very large and outside the ability of the finite precision used. Handling overflow issues requires care and accuracy is lost. The number of times this must be repeated is difficult to predict as the decay of E_{best} that appears in Algorithm 4 may plateau for many iterations before decreasing [26].

The FLP formulation as an ILP does not lend itself to an evaluation of the computational complexity directly as it depends strongly on the particular underlying algorithm and its implementation. An alternative metric that often correlates with the computational complexity of solving an ILP is the number of nonzeros that appear in the constraint matrix. The constraint matrix that appears in our ILP contains $(n + 3np)$ nonzeros, which grows at worst quadratically in n if the number of targets p grows linearly with n , thus it grows more slowly than the greedy algorithm. Our implementation which uses the GNU Linear Programming Kit [38] to solve the ILP returns a set of driver nodes faster than the greedy algorithm every time it was compared. As for the LPGM, the FLP formulation does not suffer from overflow or underflow issues during the solution of the Lyapunov equation that appears in Alg. 4 to which the LPGM heuristic is prone. The FLP method also performed considerably faster than the LPGM heuristic for all comparisons made.

REFERENCES

- [1] Alexandre Bovet and Hernán A. Makse. Influence of fake news in Twitter during the 2016 US presidential election. *Nature Communications*, 10(1):7, dec 2019.
- [2] Sergio Arianos, E Bompart, A Carbone, and Fei Xue. Power grid vulnerability: A complex network approach. *Chaos: An Interdisciplinary Journal of Nonlinear Science*, 19(1):13119, mar 2009.
- [3] Giuliano Andrea Paganini and Marco Aiello. The power grid as a complex network: a survey. *Physica A: Statistical Mechanics and its Applications*, 392(11):2688–2700, 2013.
- [4] Albert-László Barabási, Réka Albert, and Hawoong Jeong. Scale-free characteristics of random networks: the topology of the world-wide web. *Physica A: statistical mechanics and its applications*, 281(1-4):69–77, 2000.
- [5] Olaf Sporns. Structure and function of complex brain networks. *Dialogues in clinical neuroscience*, 15(3):247, 2013.
- [6] Nir Grinberg, Kenneth Joseph, Lisa Friedland, Briony Swire-Thompson, and David Lazer. Fake news on Twitter during the 2016 U.S. presidential election. *Science*, 363(6425):374–378, jan 2019.
- [7] Ying Hong Li, Pan Pan Wang, Xiao Xu Li, Chun Yan Yu, Hong Yang, Jin Zhou, Wei Wei Xue, Jun Tan, and Feng Zhu. The Human Kinome Targeted by FDA Approved Multi-Target Drugs and Combination Products: A Comparative Study from the Drug-Target Interaction Network Perspective. *PLOS ONE*, 11(11):e0165737, nov 2016.
- [8] Yang-Yu Liu and Albert-László Barabási. Control principles of complex systems. *Reviews of Modern Physics*, 88(3):35006, 2016.
- [9] Isaac Klickstein, Afroza Shirin, and Francesco Sorrentino. Locally Optimal Control of Complex Networks. *Physical Review Letters*, 119(26):268301, dec 2017.
- [10] Yang-Yu Liu, Jean-Jacques Slotine, and Albert-László Barabási. Controllability of complex networks. *Nature*, 473(7346):167–173, may 2011.
- [11] Zhengzhong Yuan, Chen Zhao, Zengru Di, Wen-Xu Wang, and Ying-Cheng Lai. Exact controllability of complex networks. *Nature Communications*, 4(1):2447, dec 2013.
- [12] Jianxi Gao, Yang-Yu Liu, Raissa M D’Souza, and Albert-László Barabási. Target control of complex networks. *Nature Communications*, 5(1):5415, dec 2014.
- [13] Francesco Lo Indice, Franco Garofalo, and Francesco Sorrentino. Structural permeability of complex networks to control signals. *Nature Communications*, 6(1):8349, dec 2015.
- [14] Xizhe Zhang, Huaizhen Wang, and Tianyang Lv. Efficient target control of complex networks based on preferential matching. *PloS one*, 12(4):e0175375, 2017.
- [15] Gang Yan, Jie Ren, Ying-Cheng Lai, Choy-Heng Lai, and Baowen Li. Controlling complex networks: How much energy is needed? *Physical review letters*, 108(21):218703, 2012.
- [16] Gang Yan, Georgios Tsekenis, Baruch Barzel, Jean-Jacques Slotine, Yang-Yu Liu, and Albert-László Barabási. Spectrum of controlling and observing complex networks. *Nature Physics*, 11(9):779–786, sep 2015.
- [17] Jie Sun and Adilson E Motter. Controllability Transition and Nonlocality in Network Control. *Physical Review Letters*, 110(20):208701, may 2013.
- [18] Isaac Klickstein, Afroza Shirin, and Francesco Sorrentino. Energy scaling of targeted optimal control of complex networks. *Nature Communications*, 8:15145, apr 2017.
- [19] Tyler H Summers, Fabrizio L Cortesi, and John Lygeros. On submodularity and controllability in complex dynamical networks. *IEEE Transactions on Control of Network Systems*, 3(1):91–101, 2016.
- [20] Vasileios Tzoumas, Mohammad Amin Rahimian, George J Pappas, and Ali Jadbabaie. Minimal actuator placement with optimal control constraints. In *2015 American Control Conference (ACC)*, pages 2081–2086. IEEE, IEEE, jul 2015.
- [21] Vasileios Tzoumas, Mohammad Amin Rahimian, George J Pappas, and Ali Jadbabaie. Minimal actuator placement with bounds on control effort. *IEEE Transactions on Control of Network Systems*, 3(1):67–78, 2016.
- [22] Alexander Olshevsky. Minimal controllability problems. *IEEE Transactions on Control of Network Systems*, 1(3):249–258, 2014.
- [23] Guoqi Li, Wuhua Hu, Gaoxi Xiao, Lei Deng, Pei Tang, Jing Pei, and Luping Shi. Minimum-cost control of complex networks. *New Journal of Physics*, 18(1):13012, 2016.
- [24] Guoqi Li, Jie Ding, Changyun Wen, and Jiangshuai Huang. Minimum Cost Control of Directed Networks With Selectable Control Inputs. *IEEE Transactions on Cybernetics*, pages 1–10, 2018.
- [25] Guoqi Li, Lei Deng, Gaoxi Xiao, Pei Tang, Changyun Wen, Wuhua Hu, Jing Pei, Luping Shi, and H Eugene Stanley. Enabling Controlling Complex Networks with Local Topological Information. *Scientific reports*, 8(1):4593, 2018.
- [26] Leitao Gao, Guangshe Zhao, Guoqi Li, Lei Deng, and Fei Zeng. Towards the minimum-cost control of target nodes in directed networks with linear dynamics. *Journal of the Franklin Institute*, 355(16):8141–8157, nov 2018.
- [27] Tyler H Summers and John Lygeros. Optimal sensor and actuator placement in complex dynamical networks. *IFAC Proceedings Volumes*, 47(3):3784–3789, 2014.
- [28] Marshall L. Fisher, George L. Nemhauser, Laurence A. Wolsey, Marshall L. Fisher, George L. Nemhauser, and Laurence A. Wolsey. An analysis of approximations for maximizing submodular set functions—II. In *Polyhedral combinatorics*, volume 14, pages 265–294. Springer, dec 1978.
- [29] Sven J Hammarling. Numerical Solution of the Stable, Non-negative Definite Lyapunov Equation Lyapunov Equation. *IMA Journal of Numerical Analysis*, 2(3):303–323, 1982.
- [30] Peter Benner and Jens Saak. Numerical solution of large and sparse continuous time algebraic matrix Riccati and Lyapunov equations: a state of the art survey. *GAMM-Mitteilungen*, 36(1):32–52, 2013.
- [31] Shiyu Zhao and Fabio Pasqualetti. Controllability Degree of Directed Line Networks: Nodal Energy and Asymptotic Bounds. In *2018 European Control Conference (ECC)*, pages 1857–1862. IEEE, jun 2018.
- [32] Isaac Samuel Klickstein and Francesco Sorrentino. Control Distance and Energy Scaling of Complex Networks. *IEEE Transactions on Network Science and Engineering*, 2018.
- [33] Isaac Klickstein, Ishan Kafle, Sudarshan Bartaula, and Francesco Sorrentino. Energy Scaling with Control Distance in Complex Networks. In *2018 IEEE International Symposium on Circuits and Systems (ISCAS)*, pages 1–5. IEEE, may 2018.

- [34] Isaac Klickstein and Francesco Sorrentino. Control Energy of Lattice Graphs. In *2018 IEEE Conference on Decision and Control (CDC)*, pages 6132–6138. IEEE, dec 2018.
- [35] Thomas Kailath. *Linear systems*. Prentice hall Englewood Cliffs, NJ, 1980.
- [36] Harry Bateman. *Tables of Integral Transforms Volume I*. McGraw-Hill Book Company, Inc, 1954.
- [37] Pitu B Mirchandani and Richard L Francis. *Discrete location theory*. John Wiley \& Sons, Inc, 1990.
- [38] Andrew Makhorin. GNU Linear Programming Kit, 2018.
- [39] Kamal Jain, Mohammad Mahdian, and Amin Saberi. A new greedy approach for facility location problems. In *Proceedings of the thiry-fourth annual ACM symposium on Theory of computing - STOC '02*, page 731, New York, New York, USA, 2002. ACM Press.
- [40] Milton Abramowitz and Irene A Stegun. *Handbook of mathematical functions: with formulas, graphs, and mathematical tables*, volume 55. Courier Corporation, 1965.
- [41] Duncan J Watts and Steven H Strogatz. Collective dynamics of 'small-world' networks. *nature*, 393(6684):440, 1998.
- [42] Guoqi Li, Jie Ding, Changyun Wen, and Jing Pei. Optimal control of complex networks based on matrix differentiation. *EPL (Europhysics Letters)*, 115(6):68005, sep 2016.
- [43] R H Bartels and G W Stewart. Solution of the matrix equation $AX + XB = C$ [F4]. *Communications of the ACM*, 15(9):820–826, sep 1972.



Isaac Klickstein received the Ph.D. degree in mechanical engineering at the University of New Mexico, Albuquerque NM, 87131, in 2020. Prior to graduating, he was a doctoral student in the Chaos Lab at UNM where he published over a dozen peer reviewed journal papers and was a member of an invited session at the 2019 SIAM Conference on Applications of Dynamical Systems. His interests include optimal control, controlling distributed networks, and dynamics on lattices.



Francesco Sorrentino received a master's degree in Industrial Engineering in 2003 and a Ph.D. in Control Engineering in 2007 both from the University of Naples Federico II (Italy). His expertise is in dynamical systems and controls, with particular emphasis on nonlinear dynamics and optimal control. His work includes studies on dynamics and control of complex dynamical networks and hypernetworks, adaptation in complex systems, sensor adaptive networks, coordinated autonomous vehicles operating in a dynamically changing environment, and identification of nonlinear systems. He is interested in applying the theory of dynamical systems to model, analyze, and control the dynamics of complex distributed energy systems, such as power networks and smart grids. Subjects of current investigation are evolutionary game theory on networks (evolutionary graph theory), the dynamics of large networks of coupled neurons, and the use of optimal control to design drug dosage schedules for biomedical applications.

He has published more than 50 papers in international scientific peer reviewed journals. He is the awardee of the National Institutes of Health Trailblazer Award from the National Institute of Biomedical Imaging and Bioengineering (NIBIB.)